Mouslopoulou, V., Nicol, A., Begg, J. G., Oncken, O., Moreno, M. (2015): Clusters of mega-earthquakes on upper-plate faults control the Eastern Mediterranean hazard. - *Geophysical Research Letters*, *42*, 23, pp. 10282—10289.

DOI: http://doi.org/10.1002/2015GL066371

AGU PUBLICATIONS

Geophysical Research Letters

RESEARCH LETTER
10.1002/2015GL066371

Key Points:
- Uplift along the Hellenic forearc transient due to earthquake clustering
- Earthquakes occur mostly on upper plate faults rather than the plate interface
- Seismic hazard in Eastern Mediterranean underestimated

Supporting Information:
- Supporting Information S1
- Table S1

Correspondence to:
V. Mouslopoulou,
vasso@gfz-potsdam.de

Citation:
Mouslopoulou, V., A. Nicol, J. Begg, O. Oncken, and M. Moreno (2015), Clusters of megaearthquakes on upper plate faults control the Eastern Mediterranean hazard, *Geophys. Res. Lett.*, *42*, 10,282–10,289, doi:10.1002/2015GL066371.

Received 28 SEP 2015
Accepted 6 NOV 2015
Accepted article online 30 NOV 2015
Published online 14 DEC 2015

Clusters of megaearthquakes on upper plate faults control the Eastern Mediterranean hazard

Vasiliki Mouslopoulou[1], Andrew Nicol[2], John Begg[3], Onno Oncken[1], and Marcos Moreno[1]

[1]German Research Centre for Geosciences, GFZ Helmholtz Centre Potsdam, Germany, [2]Department of Geological Sciences, University of Canterbury, Christchurch, New Zealand, [3]GNS Science, Lower Hutt, New Zealand

Abstract The Hellenic subduction margin in the Eastern Mediterranean has generated devastating historical earthquakes and tsunamis with poorly known recurrence intervals. Here stranded paleoshorelines indicate strong uplift transients (0–7 mm/yr) along the island of Crete during the last ~50 kyr due to earthquake clustering. We identify the highest uplift rates in western Crete since the demise of the Minoan civilization and along the entire island between ~10 and 20 kyr B.P., with the absence of uplifted Late Holocene paleoshorelines in the east being due to seismic quiescence. Numerical models show that uplift along the Hellenic margin is primarily achieved by great earthquakes on major reverse faults in the upper plate with little contribution from plate-interface slip. These earthquakes were strongly clustered with recurrence intervals ranging from hundreds to thousands of years and primarily being achieved by fault interactions. Future great earthquakes will rupture seismically quiet areas in eastern Crete, elevating both seismic and tsunami hazards.

1. Introduction

Subduction of the African plate along the Hellenic margin in the Eastern Mediterranean is primarily accommodated by steady aseismic slip of ~35–40 mm/yr on the plate interface [*Reilinger et al.*, 2006] (Figure 1). Despite the high proportion of relative plate motion taken up by aseismic slip (≥80%) [*Vernant et al.*, 2014], devastating great earthquakes ($>M8$) and associated tsunamis occur in the Hellenic forearc [*Guidoboni and Comastri*, 1997; *Papadopoulos*, 2011], with the most widely documented being the A.D. 365 M~8.5 event which uplifted western Crete by as much as 10 m [*Flemming*, 1978; *Pirazzoli et al.*, 1982, 1996; *Stiros*, 2001; *Shaw et al.*, 2008; *Papadopoulos*, 2011]. Unlike most subduction systems worldwide [*Tichelaar and Ruff*, 1993], the source of the great A.D. 365 earthquake is thought to be a reverse fault in the overriding plate rather than the subduction thrust [*Stiros and Drakos*, 2006; *Shaw et al.*, 2008; *Papadimitriou and Karakostas*, 2008; *Stiros*, 2010; *Shaw and Jackson*, 2010]. Independent of whether the 10 m of uplift in western Crete was due entirely to the A.D. 365 earthquake or to a sequence of events between A.D. 0 and 500 [*Pirazzoli et al.*, 1982, 1996; *Kelletat*, 1991; *Stiros*, 2001; *Shaw et al.*, 2008], it is clear that the uplift responsible for the presence of Crete is at least partly coseismic. Therefore, uplift of paleoshorelines in coastal Crete constrains the uplift history, providing important information on the timing and magnitude of large prehistoric earthquakes in the Hellenic forearc. These paleoshorelines are spectacularly preserved as platforms or sea notches encrusted in calcareous beachrock (see Figures S1 and S2 in the supporting information) and have been extensively studied [*Angelier et al.*, 1982; *Pirazzoli et al.*, 1982, 1996; *Shaw et al.*, 2008; *Gallen et al.*, 2014; *Strobl et al.*, 2014; *Tiberti et al.*, 2014; *Mouslopoulou et al.*, 2015]. We use the altitudes and radiocarbon ages of these paleoshorelines in combination with sea level curves to analyze, for the first time, uplift rates from the entire length of Crete over the last 50 kyr (Figure 2a). Our analysis highlights strong temporal transients in uplift rates that varied little spatially on Crete prior to the period of Minoan civilization (~2700–1450 years B.C.), despite an interpreted apparent eastward change from seismic to aseismic uplift [*Meier et al.*, 2007; *Zachariasse et al.*, 2008; *Becker et al.*, 2010; *Gallen et al.*, 2014; *Strobl et al.*, 2014].

2. Spatial and Temporal Uplift Patterns on Crete

We show that uplift rates over the last ~50 kyr were transitory and that, prior to about 3000 years B.C., did not vary from west to east along Crete (Figures 2b and 2c). We achieve this by calculating the uplift and uplift rate for 108 paleoshorelines at 31 coastal sites on Crete which are today elevated by up to 23 m above sea level (Figure 2a and Table S1).

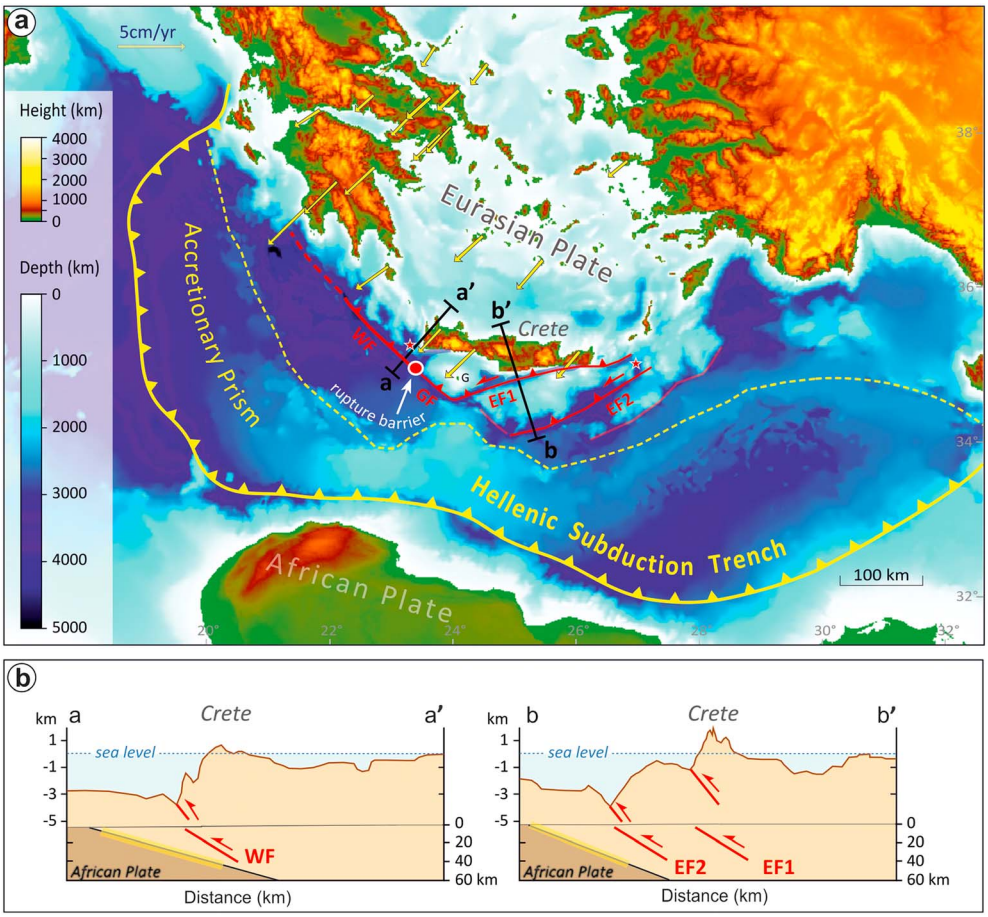

Figure 1. The Hellenic subduction margin and the main forearc faults offshore Crete. (a) Stars indicate the epicenters of the A.D. 365 (west) and A.D. 1303 (east) earthquakes in offshore Crete. Yellow arrows indicate movement vectors from permanent GPS stations [*Mouslopoulou et al*., 2014]. The northward extent of the accretionary prism is indicated by yellow dashed line. Bathymetry from GEBCO. G = Gavdos Island, WF = Western Fault, GF = Gavdos Fault, EF1 = Eastern Fault 1, EF2 = Eastern Fault 2. (b) Cross sections of the western (a-a′) and eastern (b-b′) Crete (modified from *Shaw and Jackson* [2010]). The plate interface is indicated by the black line, and the weakly locked portion of the interface is highlighted by yellow polygon. Vertical scale changes with depth.

Uplift and uplift rates (Figures 2b and 2c and Table S1) were calculated using the altitude and radiocarbon age of paleoshorelines together with the sea level curves. All radiocarbon ages (Table S1) are recalibrated using the software WinsCal v.6.0 (see online supporting information) and range from ~0.5 to 46 calibrated kyr B.P. We use global sea level curves of *Siddall et al*. [2003] for pre-Holocene paleoshorelines and the Mediterranean sea level curve of *Antonioli et al*. [2007] for post ~3000 years B.C. data. The *Antonioli et al*. [2007] curve predicts sea level rise at a uniform rate of ~1 m/1000 years since 2000 years B.C. and a total of 6–7 m since ~3000 years B.C., which is consistent with the drowning of many archeological sites throughout the Mediterranean [*Antonioli et al*., 2007; *Auriemma and Solinas*, 2009; *Mouslopoulou et al*., 2015], and with the reverse age order (i.e., youngest shorelines are highest) of 0–3000 years B.C. paleoshorelines at the majority of sites in western Crete [*Pirazzoli et al*., 1996; *Mouslopoulou et al*., 2015] (Figure S1a and Table S1). Sensitivity tests suggest that the first-order uplift estimates presented here are independent of which sea level curves were employed and, in particular, the rate of Late Holocene sea level rise of the Mediterranean.

The age-altitude relationships of paleoshorelines and their associated stratigraphy are different in the west and east of Crete (Table S1 and Figure S1). To the west, paleoshorelines up to 8 m above present sea level mainly range in age up to 3000 years B.C., while higher marine platforms are 20–40 kyr and increase in age with altitude [*Mouslopoulou et al*., 2015] (Table S1 and Figure S1a). These ages contrast with eastern parts of Crete where no Late Holocene paleoshorelines have been recorded and the ages of marine platforms

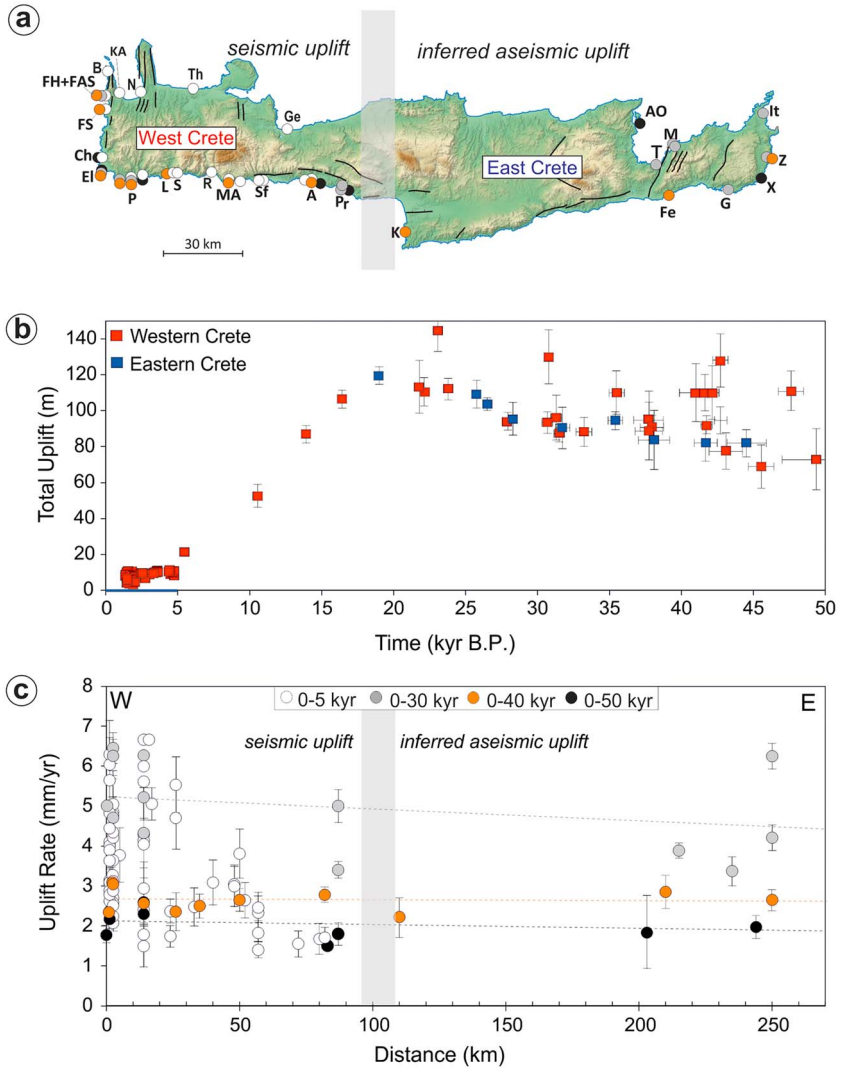

Figure 2. Locality map of paleoshoreline uplift and uplift rate data along Crete during the last 50 kyr. (a) Letters show locations of the individual study sites presented in Table S1. Localities are color coded according to the interval over which uplift rates were measured in Figure 2c (i.e., white-filled circles 0–5 kyr, grey-filled circles 0–30 kyr, orange-filled circles 0–40 kyr, and black-filled circles 0–50 kyr). (b) Total uplift on western and eastern Crete during the last 50 kyr. (c) Uplift rates along Crete for the last 50 kyr averaged over the color-coded periods of time. See Figure 2a for localities. Color-coded best fit lines indicate uniform, but transitory, uplift rate along Crete and across the inferred boundary between seismic and aseismic uplift. Slight eastward tilt on the 0–30 kyr best fit line reveals the impact of the A.D. 365 earthquake. Ge = Georgioupoli, Th = Thodorou, N = Nopigia, KA = Kalyviani, B = Balos, FH = Falasarna-Harbour, FAS = Falasarna, FS = Falasarna-South, Ch = Chrysoskalittsa, El = Elafonisi, P = Paleochora, R = Roumeli, L = Lissos, S = Sougia, Ma = Marmara, Sf = Sfakia, A = Amoudi, Pr = Preveli, K = Kommos, Fe = Ferma, G = Goudouras, X = Xerokampos, Z = Zakros, It = Itanos, M = Mochlos, T = Tholos, and AO = Ancient-Olous. For details see Table S1.

within 10 m of sea level range from ~20 to 45 kyr (Figure S1b), again increasing in age with altitude [*Mouslopoulou et al.*, 2015]. Changes in the ages and altitudes of paleoshorelines from west to east are mainly due to Late Holocene coseismic uplift in the western parts of the island which, if backstripped or removed from the uplift patterns, lowers all paleoshorelines of 20–40 kyr age to within 20 m of the present sea level [*Mouslopoulou et al.*, 2015]. Therefore, prior to 3000 years B.C., the timing and magnitudes of changes in uplift rates were comparable along Crete's entire coastline and did not change across the inferred boundary [*Meier et al.*, 2007; *Zachariasse et al.*, 2008; *Shaw et al.*, 2008; *Becker et al.*, 2010; *Gallen et al.*, 2014; *Strobl et al.*, 2014] between seismic uplift in the west and aseismic uplift to the east (Figures 2a and 2c). This uniformity applies for uplift rates averaged over 0–30, 0–40, and 0–50 kyr (Figure 2c). Over shorter time intervals the rates of

time-averaged uplift at individual sites are transient, being greatest (up to 7 mm/yr) for paleoshorelines of younger than 2000 years and ~10–20 kyr in age, with little or no measureable uplift from 0 to 3000 years B.C. and 20–50 kyr (Figures 2b and 2c). Accelerated rates of uplift between ~5 and 20 kyr occurred in eastern and western parts of the island. These transitory rates are at odds with the constant rates of plate convergence [*Reilinger et al*. 2006; *Vernant et al*., 2014] and require explanation.

3. Mechanism for Uplift Transients

Historical accounts and archeological investigations support the view that western Crete was raised in a discrete uplift event, which was accompanied by a tsunami and has been widely attributed to a great earthquake [*Flemming*, 1978; *Pirazzoli et al*., 1982, 1996; *Stiros*, 2001; *Shaw et al*., 2008; *Papadopoulos*, 2011]. No such Holocene earthquakes have been recorded by the paleoshorelines of eastern Crete, although the tsunamigenic A.D. 1303 ~*M*8 earthquake is inferred to have ruptured the eastern Hellenic margin, approximately 50–60 km offshore southeast of Crete [*Guidoboni and Comastri*, 1997; *Papadopoulos*, 2011] (Figure 1). The absence of evidence for coseismic uplift in eastern Crete has contributed to the view that this part of the Hellenic margin is being uplifted mainly aseismically [*Meier et al*., 2007; *Zachariasse et al*., 2008; *Becker et al*., 2010; *Gallen et al*., 2014; *Strobl et al*., 2014]. Aseismic uplift has been ascribed to a number of mechanisms including, sediment underplating [*Angelier et al*., 1982; *Gallen et al*., 2014; *Strobl et al*., 2014], return flow of lithospheric material from the subduction channel [*Meier et al*., 2006; *Becker et al*., 2010] and isostatic adjustments to mass deficit beneath Crete [*Snopek et al*., 2007]. While these mechanisms are capable of producing uplift [e.g., *Wilson et al*., 2007], over thousands to tens of thousands of years they are generally regarded to be steady state [*Gallen et al*., 2014; *Zachariasse et al*., 2008] and cannot be called upon to directly produce uplift transients that span as little as a few thousand years. The similarity of long-term uplift rates across the island (i.e., in areas inferred to be experiencing seismic and aseismic uplift; Figure 2c) together with the Late Holocene seismic uplift in the west of Crete [*Pirazzoli et al*., 1982, 1996; *Stiros*, 2001; *Shaw et al*., 2008] and the A.D. 1303 seismic slip southeast of Crete [*Guidoboni and Comastri*, 1997; *Papadopoulos*, 2011] strongly supports the view that coastal uplift of eastern Crete may also be seismogenic.

We propose that uplift of Crete is primarily achieved by coseismic slip on reverse faults in the overriding plate (see WF, GF, and EF1 faults in Figure 1) with uplift transients being due to order of magnitude changes of displacement rates on these faults. For such a model the absence of evidence for uplift events in eastern Crete reflects the fact that the area has been seismically quiescent during the Late Holocene (similar to western Crete for the time period 2 to 5 kyr), as opposed to the more generally held view that uplift is largely aseismic [*Meier et al*., 2007; *Zachariasse et al*., 2008; *Becker et al*., 2010; *Gallen et al*., 2014; *Strobl et al*., 2014].

To test the seismic fault slip idea, the spatial pattern of uplift from paleoshoreline observations has been compared to the output from a numerical finite element model that simulates elastic deformation due to fault slip (Figure 3). Our model assumes that all deformation responsible for the uplift of the paleoshorelines is due to fault slip and does not include viscoelastic and plastic deformation. However, the viscoelastic/permanent deformation, if any, may only account for 20–30% of the coseismic moment release [*Melbourne et al*., 2002], and thus, its noninclusion does not impact on the first-order conclusions drawn by this study. The model comprises faults in western (WF and GF) and eastern (EF1 and EF2) segments of the Hellenic forearc (Figures 1, 3, and S3). The geometries of these faults are constrained by seismic-reflection data, focal mechanisms, receiver-function data, and previous dislocation modeling [*Jackson*, 1994; *Sodoudi et al*., 2006; *Shaw et al*., 2008; *Stiros*, 2010; *Shaw and Jackson*, 2010; *Kokinou et al*., 2012]. The faults are modeled to intersect the plate interface at ~40 km depth, dip 40° to the north and reach the seabed along sharp bathymetric troughs offshore west and south of Crete (Figure 1). Matching the Late Holocene uplift in western Crete, including the absence of uplift on Gavdos Island south of Crete [*Pirazzoli et al*., 1982, 1996], requires up to 23 m of slip on fault WF (Figures 3a and S4), with rupture on this fault terminating near the longitude of the west coast (~23.5°E) and ~15 km south of Crete, in agreement with previous models [*Stiros and Drakos*, 2006; *Shaw et al*., 2008; *Papadimitriou and Karakostas*, 2008; *Stiros*, 2010]. Approximately uniform uplift and uplift rates along Crete (Figures 3c and 3d), as indicated by palaeoshorelines (Figure 2c), are produced by our model when slip on three of these faults (WF, GF, and EF1) is aggregated. While changes in topography across faults in the overriding plate suggest that these structures locally influence uplift, they are not required in the model to match the first-order uplift patterns. Sensitivity tests show that uniform slip along Crete could

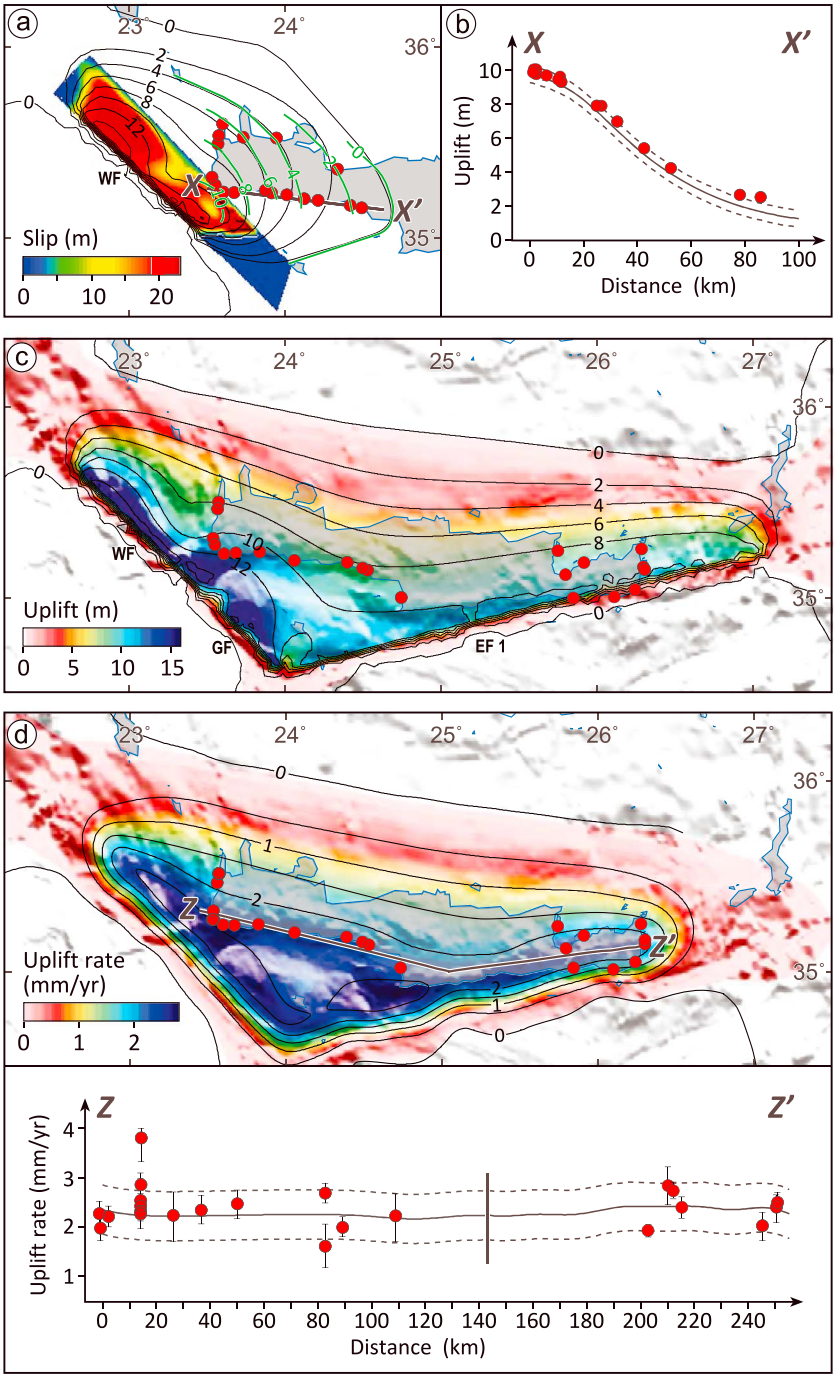

Figure 3. Modeling of the spatial distribution of uplift and uplift rate due to slip on reverse faults offshore Crete. (a) Measured (green) versus modeled (black) contours of uplift on western Crete due to Late Holocene slip on WF. Contours of uplift calculated by best fit numerical elastic finite element model. (b) Modeled uplift (black line with dashed lines showing 2σ uncertainties) is compared to uplift measured at localities along the X-X′ profile. (c) Modeled cumulative uplift on Crete produced by slip on the WF, GF, and EF1 faults. (d) Map illustrating the predicted 50 kyr uplift rate on Crete after numerous earthquake cycles. Modeled uplift rates (black line with dashed lines showing 2σ uncertainties) are compared with the measured (in the field) 40–50 kyr rates along the profile Z-Z′. Vertical line marks the bend in the profile.

not be reproduced without rupture on both the GF and EF1 segments, in addition to WF (see online supporting information) (Figure S5b, S6a, and S6b). Maximum slip on GF and EF1 are 10 and 15 m, respectively (Figures S5a and S5c), smaller than that on WF (23 m) and consistent with the shorter length and distance from the land, respectively, of these faults (compared to WF).

Our analysis of paleoshorelines and numerical modeling indicates that the reverse faults modeled to be responsible for the uplift of Crete had displacement rates of 4 ± 0.5 mm/yr over the last 50 kyr (Figure S7b). These displacement rates are a small fraction (~10%) of the total relative plate motion of 35–40 mm/yr. Nevertheless, they represent at least ~50% (and up to 100%) of the ~3.5–8 mm/yr total convergence that is being stored elastically [*Reilinger et al*. 2006; *Vernant et al*., 2014] and partly released during subsequent earthquakes that rupture the interseismically locked section of the plate interface south of Crete [*Shaw et al*., 2008; *Vernant et al*., 2014] (Figure 1b). The interseismically locked portion of the interface has a low dip (e.g., 17–20°) [*Meier et al*., 2007], and our modeling suggests that its slip is not likely to produce significant uplift of Crete. The reverse faults modeled in Figure 3 splay from the plate interface down dip of the interseismically locked zone in a region of elevated shear stress, which is common along subduction margins globally [*Nicol and Beavan*, 2003; *Rosenau and Oncken*, 2009], and are inferred to be loaded by slip during large earthquakes on the plate interface. Transient uplift rates suggest that transfer of slip from the subducting to the overriding plate is most likely not uniform which could reflect a number of processes including, temporal changes in frictional properties of the subduction thrust, and overlying reverse faults, variability in the stress interactions between the faults and/or temporal changes in the strain partitioning between the plate interface and the upper plate faults [*Wech and Creager*, 2008; *Rosenau and Oncken*, 2009]. Our preferred explanation for the uplift transients is the latter in conjunction with fault interactions in the upper plate. Displacement rates on the upper plate faults, for example, were ~3 times faster (i.e., 12 ± 2 mm/yr) between 5 and 20 kyr B.P. compared to the average from 0 to 50 kyr B.P. (i.e., 4 ± 0.5 mm/yr). From 5 to 20 kyr upper plate faults in the Hellenic margin were accommodating ~30% of the total convergence rate (35–40 mm/yr) consistent with temporal variations in the partitioning of slip between upper plate faults and the subduction interface, leading to temporally variable interseismic strain accumulation on upper plate faults. Similar temporal fluctuations in fault strength and changes in stress loading arising from fault interactions have been proposed to account for variations in slip rates on faults in a variety of tectonic settings [*Weldon et al*., 2004; *Nicol et al*., 2006; *Mouslopoulou et al*., 2009, 2012; *Ferry et al*., 2011; *Cowie et al*., 2012] and are independent of sea level fluctuations [*Nicol et al*., 2009; *Hampel et al*., 2010]. Irrespective of the mechanisms that account for the observed variations, transient fault displacement rates have important implications for estimates of earthquake recurrence intervals and seismic hazard [*Goldfinger et al*., 2013].

4. Are Earthquake and Tsunami Hazards in Eastern Mediterranean Underestimated?

Great earthquakes and associated tsunamis along the Hellenic margin represent an important hazard for communities in the Eastern Mediterranean [*Shaw et al*., 2008]. Reverse faults in the overriding plate beneath Crete contribute significantly to this hazard. In western Crete the recurrence interval between great earthquakes, similar in size and location to that reported for the A.D. 365 event, was ~5–8 kyr [*Shaw et al*., 2008; *Vernant et al*., 2014]. Here we show that, in addition to the western Hellenic margin, the eastern margin is also seismogenic. Our analysis suggests that for the portion of the Hellenic margin straddled by Crete, the rate of occurrence of magnitude >8 earthquakes on individual faults may have been highly variable. For example, the fault WF beneath western Crete ruptured every 4.5 kyr when averaged over the last 50 kyr, as frequently as every 1.5 kyr between 5 and 20 kyr, and not at all between 0 and 3000 years B.C. (Table S2).

Our paleoshoreline uplift data and fault numerical model are consistent with 10 to 20 great earthquakes on each reverse fault (i.e., WF, GF, and EF1) over the last 50 kyr (Table S2). These numbers of events are considered to be a minimum as the 10 m of maximum uplift, on which the modeling of all faults is anchored (see online supporting information), assumes that the Late Holocene uplift of western Crete occurred in a single earthquake (as opposed to multiple events) (Figure 3a). In addition, megathrust events on the weakly locked interplate were not included in our calculations because they contribute little to the observed uplift, although, such events likely accommodated up to 50% of the strain that is stored elastically over the last 50 kyr. Taking all modeled faults together the recurrence interval for great earthquakes along the Hellenic

margin in Crete is about 1300 years (Table S2), significantly shorter than the recurrence interval for individual faults but longer than the ~800 years calculated for the entire Hellenic subduction margin by *Shaw et al.* [2008].

The elapsed time of ~1650 years since the A.D. 365 earthquake is comparable to the ~1300 years recurrence interval for all three faults in our model over the last 50 kyr (Table S2). While this similarity of elapsed time and averaged earthquake recurrence interval may be interpreted to indicate high seismic and tsunami hazards, estimates of hazards should incorporate the order-of-magnitude temporal changes in recurrence intervals. In contrast to most subduction margins globally, great earthquakes in the Hellenic margin are strongly clustered in time and while we are presently experiencing a seismically quiet period, future great earthquakes can be expected beneath both eastern and western Crete, although fluctuations in recurrence intervals mean that forecasting these events represents a challenge.

Acknowledgments
This work has been supported by section 3.1 of the German Centre of Geosciences (GFZ) and a bilateral grant of the Federal Ministry of Education and Research of Germany (BMBF) and the Royal Society of New Zealand. The reported data are summarized in Table S1 in the supporting information. The raw data in this table were derived from *Pirazzoli et al.* [1996], *Shaw et al.* [2008], *Strasser et al.* [2011], *Tiberti et al.* [2014], and *Mouslopoulou et al.* [2015]. The article was benefited by constructive comments from Philippe Vernant, an anonymous reviewer, and the journal Editor A. Newman, all of whom are gratefully acknowledged.

References

Aagaard, B. T., M. G. Knepley, and C. A. Williams (2013), A domain decomposition approach to implementing fault slip in finite-element models of quasi-static and dynamic crustal deformation, *J. Geophys. Res. Solid Earth*, *118*, 3059–3079, doi:10.1002/jgrb.50217.

Angelier, J., N. Lybéris, X. Le Pichon, E. Barrier, and P. Huchon (1982), The tectonic development of the Hellenic arc and the Sea of Crete: A synthesis, *Tectonophysics*, *86*, 159–196.

Antonioli, F., et al. (2007), Sea-level change during the Holocene in Sardinia and in the northeastern Adriatic (central Mediterranean Sea) from archaeological and geomorphological data, *Quat. Sci. Rev.*, *26*, 2463–2486.

Auriemma, R., and E. Solinas (2009), Archaeological remains as sea level change markers: A review, *Quat. Int.*, *206*, 134–146.

Becker, D., T. Meier, M. Bohnhoff, and H.-P. Harjes (2010), Seismicity at the convergent plate boundary offshore Crete, Greece, observed by an amphibian network, *J. Seismol.*, *14*, 369–392.

Cowie, P. A., G. P. Roberts, J. M. Bull, and F. Visini (2012), Relationships between fault geometry, slip rate variability and earthquake recurrence in extensional settings, *Geophys. J. Int.*, *189*, 143–160.

Ferry, M., M. Meghraoui, N. Abou Karaki, M. Al-Taj, and L. Khalil (2011), Episodic behavior of the Jordan Valley section of the Dead Sea fault inferred from a 14-ka-long integrated catalog of large earthquakes, *Bull. Seismol. Soc. Am.*, *101*, 39–67.

Flemming, N. (1978), Holocene eustatic changes and coastal tectonics in the Northeast Mediterranean: implications for models of crustal consumption, *Trans. R. Soc. London*, *289*, 405–458.

Gallen, S., K. W. Wegmann, D. R. Bohnenstiehl, F. J. Pazzaglia, M. T. Brandon, and C. Fassoulas (2014), Active simultaneous uplift and margin-normal extension in a forearc high, Crete, Greece, *Earth Planet. Sci. Lett.*, *398*, 11–24.

Goldfinger, C., Y. Ikeda, R. S. Yeats, and J. Ren (2013), Superquakes and supercycles, *Seismol. Res. Lett.*, *48*, 24–32.

Guidoboni, E., and A. Comastri (1997), The large earthquake of 8 August 1303 in Crete: Seismic scenario and tsunami in the Mediterranean area, *J. Seismol.*, *1*, 55–72.

Hampel, A., T. Karow, G. Maniatis, and R. Hetzel (2010), Slip rate variations on faults during glacial loading and postglacial unloading: Implications for the viscosity structure of the lithosphere. In: C. Pascal, I.S. Stewart, B.L.A. Vermeersen, Neotectonics, Seismicity and Stress in Glaciated Regions, *J. Geol. Soc. London*, *167*, 385–399.

Jackson, J. (1994), Active tectonics of the Aegean region, *Annu. Rev. Earth Planet. Sci.*, *22*, 239–271.

Kelletat, D. (1991), The 1550 BP tectonic event in the Eastern Mediterranean as a basis for assessing the intensity of shore processes, *Z. Geomorphol.*, *81*, 181–194.

Kokinou, E., A. Tiago, and K. Evangelos (2012), Structural decoupling in a convergent forearc setting (southern Crete, Eastern Mediterranean), *Geol. Soc. Am. Bull.*, *124*, 1352–1364.

Laborel, J., C. Morhange, R. Lafont, J. L. Campion, F. Laborel-Deguen, and S. Sartoretto (1994), Biological evidence of sea-level rise during the last 4500 years on the rocky coasts of continental southwestern France and Corsica, *Mar. Geol.*, *120*, 203–223.

Meier, T., D. Becker, B. Endrun, M. Bohnhoff, B. Stöckhert, and H.-P. Harjes (2007), A model for the Hellenic subduction zone in the area of Crete based on seismological investigations, *Geol. Soc. London*, *291*, 183–199.

Melbourne, T. I., F. H. Webb, J. M. Stock, and C. Reigber (2002), Rapid postseismic transients in subduction zones from continuous GPS, *J. Geophys. Res.*, *107*(B10), 2241, doi:10.1029/2001JB000555.

Mouslopoulou, V., J. J. Walsh, and A. Nicol (2009), Fault displacement rates over a range of timescales, *Earth Planet. Sci. Lett.*, *278*, 186–197.

Mouslopoulou, V., A. Nicol, J. J. Walsh, J. G. Begg, D. B. Townsend, and D. T. Hristopulos (2012), Fault-slip accumulation in an active rift over thousands to millions of years and the importance of paleoearthquake sampling, *J. Struct. Geol.*, *36*, 71–80.

Mouslopoulou, V., V. Saltogianni, M. Gianniou, and S. Stiros (2014), Geodetic evidence for tectonic activity on the Strymon Fault System, northeast Greece, *Tectonophysics*, *633*, 246–255.

Mouslopoulou, V., J. G. Begg, A. Nicol, O. Oncken, and C. Prior (2015), Formation of Late Quaternary paleoshorelines in Crete, Eastern Mediterranean, *Earth Planet. Sci. Lett.*, *431*, 294–307, doi:10.1016/j.epsl.2015.09.007.

Nicol, A., and J. Beavan (2003), Shortening of an overriding plate and its implications for slip on a subduction thrust, central Hikurangi Margin, New Zealand, *Tectonics*, *22*(6), 1070, doi:10.1029/2003TC001521.

Nicol, A., J. J. Walsh, K. Berryman, and P. Villamor (2006), Interdependence of fault displacement rates and paleoearthquakes in an active rift, *Geology*, *34*, 865–868.

Nicol, A., J. J. Walsh, V. Mouslopoulou, and P. Villamor (2009), Earthquake histories and Holocene acceleration of fault displacement rates, *Geology*, *37*, 911–914, doi:10.1130/G25765A.1.

Papadimitriou, E., and V. Karakostas (2008), Rupture model of the great AD 365 Crete earthquake in the southwestern part of the Hellenic Arc, *Acta Geophys.*, *56*, 293–312.

Papadopoulos, G. (2011), *A Seismic History of Crete*, 416 pp., Oselotos, Athens, Greece.

Pirazzoli, P. A., J. Thommeret, Y. Thommeret, J. Laborel, and L. Montagionni (1982), Crustal block movements from Holocene shorelines: Crete and Antikythira (Greece), *Tectonophysics*, *68*, 27–43.

Pirazzoli, P. A., J. Laborel, and S. C. Stiros (1996), Earthquake clustering in the Eastern Mediterranean during historical times, *J. Geophys. Res.*, *101*(B3), 6083–6097.

Reilinger, R. E., et al. (2006), GPS constraints on continental deformation in the Africa-Arabia-Eurasia continental collision zone and implications for the dynamics of plate interactions, *J. Geophys. Res.*, *111*, B05411, doi:10.1029/2005JB004051.
Reimer, P. J., and F. G. McCormac (2002), Marine radiocarbon reservoir corrections for the Mediterranean and Aegean Seas, *Radiocarbon*, *44*, 159–166.
Reimer, P. J., and R. W. Reimer (2001), A marine reservoir correction database and on-line interface, *Radiocarbon*, *43*, 461–463.
Reimer, P. J., et al. (2013), IntCal13 and Marine13 radiocarbon age calibration curves 0–50,000 years cal BP, *Radiocarbon*, *55*, 1869–1887.
Rosenau, M., and O. Oncken (2009), Fore-arc deformation controls frequency-size distribution of megathrust earthquakes in subduction zones, *J. Geophys. Res.*, *114*, B10311, doi:10.1029/2009JB006359.
Shaw, B., and J. Jackson (2010), Earthquake mechanisms and active tectonics of the Hellenic subduction zone, *Geophys. J. Int.*, *181*, 966–984.
Shaw, B., N. N. Ambraseys, P. C. England, M. A. Floyd, G. J. Gorman, T. F. G. Higham, J. A. Jackson, J. M. Nocquet, C. C. Pain, and M. D. Piggott (2008), Eastern Mediterranean tectonics and tsunami hazard inferred from the AD 365 earthquake, *Nat. Geosci.*, *1*, 268–276.
Siddall, M., E. J. Rohling, A. Almogi-Labin, C. Hemleben, D. Meischner, I. Schmelzer, and D. A. Smeed (2003), Sea-level fluctuations during the last glacial cycle, *Nature*, *423*, 853–858.
Sivan, D., U. Schattner, C. Morhange, and E. Boaretto (2010), What can a sessile mollusk tell about neotectonics?, *Earth Planet. Sci. Lett.*, *296*, 451–458.
Snopek, K., T. Meier, B. Endrun, M. Bohnhoff, and U. Casten (2007), Comparison of gravimetric and seismic constraints on the structure of the Aegean lithosphere in the forearc of the Hellenic subduction zone in the area of Crete, *J. Geodyn.*, *44*, 173–185.
Sodoudi, F., R. Kind, D. Hatzfeld, K. Priestley, W. Hanka, K. Wylegalla, G. Stavrakakis, A. Vafidis, H. P. Harjes, and M. Bohnhoff (2006), Lithospheric structure of the Aegean obtained from *P* and *S* receiver functions, *J. Geophys. Res.*, *111*, B12307, doi:10.1029/2005JB003932.
Spratt, T. A. B. (1865), *Travels and Researchers in Crete*, vol. 2, J. van Voorst, London.
Stiros, S. (2001), The AD 365 Crete earthquake and possible seismic clustering during the fourth to sixth centuries AD in the Eastern Mediterranean: A review of historical and archaeological data, *J. Struct. Geol.*, *23*, 545–562.
Stiros, S. (2010), The 8.5+ magnitude, AD 365 earthquake in Crete: Coastal uplift, topography changes and archaeological and historical signature, *Quat. Int.*, *216*, 54–63.
Stiros, S., and A. Drakos (2006), A fault-model for the tsunami-associated, magnitude ≥8.5 Eastern Mediterranean, AD365 earthquake, *Z. Geomorphol.*, *146*, 125–137.
Strasser, T. F., C. Runnels, K. Wegmann, E. Panagopoulou, F. Mccoy, C. Digregorio, P. Karkanas, and N. Thompson (2011), Dating Palaeolithic sites in southwestern Crete, Greece, *J. Quat. Sci.*, *26*, 553–560.
Strobl, M., R. Hetzel, C. Fassoulas, and P. W. Kubik (2014), A long-term rock uplift rate for eastern Crete and geodynamic implications for the Hellenic subduction zone, *J. Geodyn.*, *78*, 21–31.
Tiberti, M. M., R. Basili, and P. Vannoli (2014), Ups and downs in western Crete (Hellenic subduction zone), *Sci. Rep.*, *4*(5677), 1–7.
Tichelaar, B. W., and L. J. Ruff (1993), Depth of seismic coupling along subduction zones, *J. Geophys. Res.*, *98*(B2), 2017–2037.
Vernant, P., R. Reilinger, and S. McClusky (2014), Geodetic evidence for low coupling on the Hellenic subduction plate interface, *Earth Planet. Sci. Lett.*, *385*, 122–129.
Wech, A. G., and C. Creager (2008), A continuum of stress, strength and slip in the Cascadia subduction zone, *Nat. Geosci.*, *4*, 624–628.
Weldon, R. J., K. M. Scharer, T. E. Fumal, and G. P. Biasi (2004), Wrightwood and the earthquake cycle: What a long recurrence record tell us about how faults work, *Geol. Soc. Am. Today*, *14*(9), doi:10.1130/1052-5173.
Wilson, K., K. Berryman, U. Cochran, and T. Little (2007), Holocene coastal evolution and uplift mechanisms of the northeastern Raukumara Peninsula, North Island, New Zealand, *Quat. Sci. Rev.*, *26*, 1106–1128.
Zachariasse, W. J., D. J. J. van Hinsbergen, and A. R. Fortuin (2008), Mass wasting and uplift on Crete and Karpathos during the early Pliocene related to initiation of south Aegean left-lateral, strike-slip tectonics, *Geol. Soc. Am. Bull.*, *120*, 976–993.